LASER-COOLED RB CLOCKS

Chad Fertig, Ron Legere, Wenko Süptitz, and Kurt Gibble,
Yale University, New Haven, CT 06511

Introduction

The most serious systematic error in laser-cooled clocks is the frequency shift due to cold collisions. Tiesenga *et al.* first calculated this shift[1] and Gibble and Chu[2] measured the shift for laser-cooled Cs clocks to be $\delta\nu/\nu = -1.7\times10^{-12}$ at a density of 10^9 cm^{-3}. Due to Cs_2 molecular bound states near zero energy, the frequency shift cross section has nearly the maximal value of $\lambda_{dB}^2/2\pi$ where λ_{dB} is the de Broglie wavelength. This large cross section led us to examine clocks based on other atoms, for which the cold collision shift might be smaller.[3,4]

In this paper, we present a preliminary measurement of the cold collision shift for ^{87}Rb where we find the shift to be more than a factor of 10 smaller than that of a laser-cooled Cs clock. We also discuss calculations for ^{85}Rb and demonstrate a juggling fountain. Juggling fountain clocks can achieve higher stability without requiring large improvements in the local oscillator. In this first Cs juggling experiment, we study the effects of collisions between juggled balls of atoms.

Laser-Cooled Rb Clock

Our laser-cooled Rb fountain clock prototype is shown in Fig. 1. Our all-solid-state laser system consists of a frequency-stabilized external-cavity grating diode laser that injects six slave lasers, one for each trapping beam. We collect as many as 5×10^{10} atoms in the vapor cell MOT[5] and then launch the ^{87}Rb atoms at a temperature of 1.85 μK in a frame moving at 3-4 m/s.

We prepare nearly 50% of the atoms in the $|F=1,m=0\rangle$ clock state using the 2 TE_{102} selection cavities. After launching, we first optically pump the atoms into the F=1 state using light tuned to the $6S_{1/2}$ F=2 → $6P_{3/2}$ F′=1′ transition. The first selection cavity transfers the atoms from the $|F=1,m=0\rangle$ state to the $|2,0\rangle$ state. A laser tuned to the $6S_{1/2}$ F=1 → $6P_{3/2}$ F′=2′ transition optically pumps the atoms remaining in F=1 thereby increasing the population in the $|2,0\rangle$ state. The 2nd cavity transfers the population in the $|2,0\rangle$ state to the $|1,0\rangle$ state. We then clear away the atoms in the $|F=2,m\neq0\rangle$ states by scattering several thousand photons from a laser beam tuned to the $6S_{1/2}$ F=2 → $6P_{3/2}$ F′=3′ cycling transition.

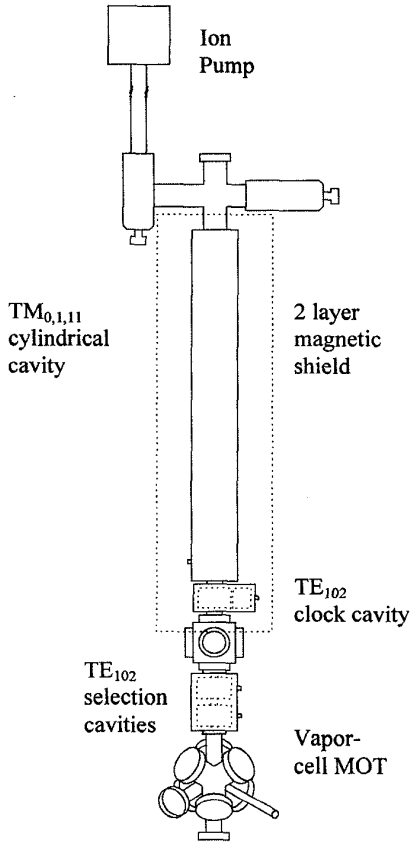

Fig. 1. Schematic of ^{87}Rb fountain clock.

Ramsey fringes for a 30 cm tall fountain are shown in Fig. 2. With a linewidth of 1 Hz and a signal-to-noise of 120:1 (limited by the local oscillator), the short-term stability is $\sigma_y(\tau) = 4\times10^{-13}\,\tau^{-1/2}$. The center frequency in Fig. 2 is at

0-7803-4373-5/98/$10.00 © 1998 IEEE

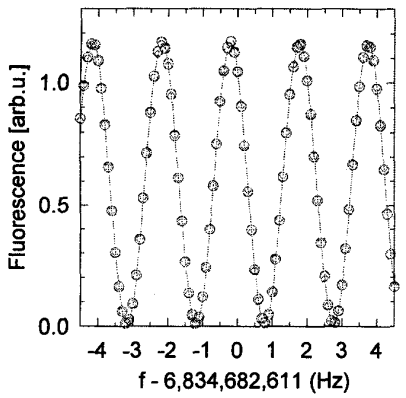

Fig. 2. ^{87}Rb Ramsey fringes. The large circles are the data and the small represent a fit to the data. The linewidth is 1 Hz and the S/N=120.

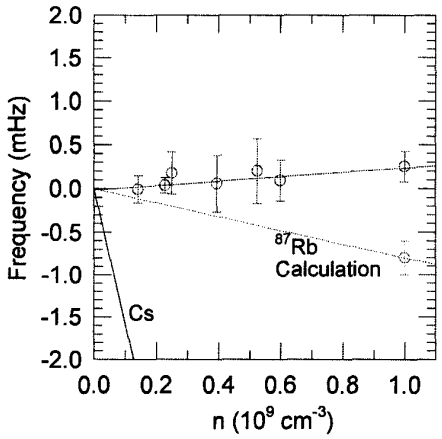

Fig. 3. ^{87}Rb clock frequency versus density for time-averaged densities up to 6×10^8 cm^{-3}. The points plotted at 10^9 cm^{-3} show the fitted uncertainty and the theoretically predicted shift and its error bar. The shift for Cs is also shown.

6,834,682,610.9 Hz and the accuracy of this is limited by the accuracy of our GPS-slaved reference oscillator. This is consistent with the frequency measured by Simon *et al.*[6] The magnetic bias field is 710 μG throughout the cavity and flight region which we can probe by exciting a Δm=1 (sigma) transition in the cylindrical $TM_{0,1,11}$ cavity. This produces a quadratic Zeeman shift of $\delta\nu/\nu = 4\times10^{-14}$.

To measure the cold collision shift for ^{87}Rb, we vary the atomic density by varying the strength of the microwave field in the 2nd state selection cavity. In Fig. 3, we show preliminary measurements of the frequency versus density and a fit to the data. Presently, the shift is non-zero by just more than the statistical error bar and it does not agree with the predicted shift.[4] We are currently experimentally testing for systematic errors in the measurement. However, our preliminary search for systematic errors shows no errors the size of the cold collision shift for Cs so that it is already clear the collision shift for Rb is at least a factor of 10 smaller than that for Cs.

For ^{85}Rb, the calculated shifts are more interesting. We predict[3] that the frequency shift produced by the population in the $|F=3,m=0\rangle$ state is +45 mHz at $n=10^9$ cm^{-3} and, for the $|F=2,m=0\rangle$, −5 mHz. By adjusting the strength of the first microwave pulse, one can vary the population ratio of the 2 clock states in the fountain to cancel the cold collision shift.[3] Using this method, the extrapolation of the shift to zero density doesn't rely on accurate measurements of density ratios and may potentially allow much higher clock stability and accuracy.

Juggling Clocks

One can achieve higher stabilities and eliminate the dead time (reducing the requirements for the local oscillator) by *juggling* atoms in the fountain as shown in Fig. 4. If, on a single launch, one could achieve a S/N = 10^4, the frequency uncertainty would be $\delta\nu/\nu = \Delta\nu/\pi\,\nu$ S/N = 5×10^{-15}. If the cycle time is 1 s, then $\sigma_y(\tau) = 5\times10^{-15}\,\tau^{-1/2}$. By launching atoms at a rate of 30 s^{-1}, we eliminate the dead time and achieve a short-term stability of $\sigma_y(\tau) = 8.5\times10^{-16}\,\tau^{-1/2}$. This improvement is achieved without the technical difficulty of achieving higher S/N and higher atomic densities. There are 2 important problems: 1) shutters, as shown in Fig. 4., must be used to block the trapping and cooling light from the interrogation region of the clock; 2) collisions between balls of atoms mandate that the launching rate be limited to about 30 s^{-1}. For higher launch rates, the frequency shift cross-section for collisions between balls increases and these may then limit the clock's accuracy and long-term stability.

We have recently demonstrated a juggling Cs fountain and have studied collisions between 2 balls of atoms. In this experiment we observe the velocity changes rather than a phase shift of an atomic coherence. We launch 2 balls of atoms from a MOT at the same velocity. The relative

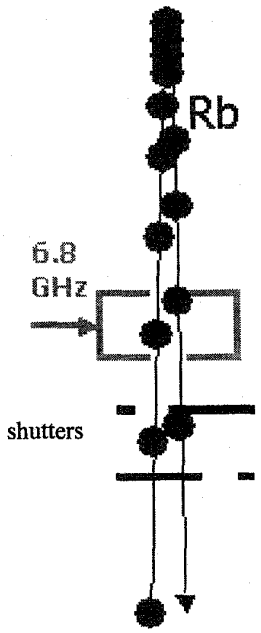

Fig. 4. Schematic for a juggling fountain clock. Balls of laser-cooled atoms are launched faster than the flight time above the microwave cavity.

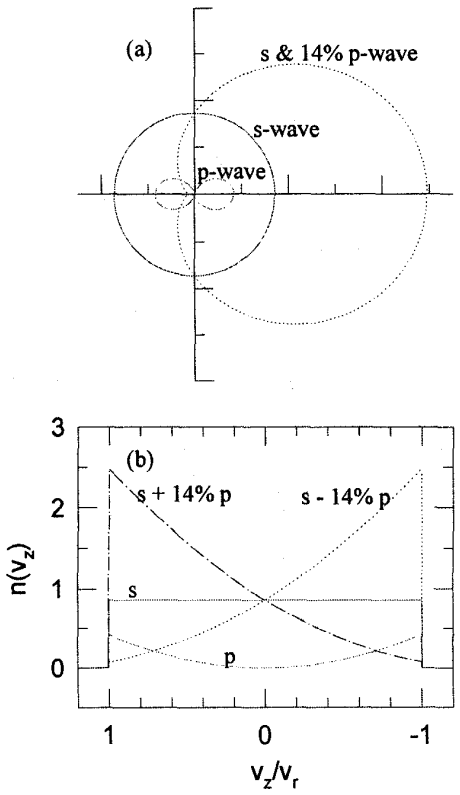

Fig. 5. (a) Angular distribution of s-wave scattering (solid), p-wave (dashed), and for coherent scattering of s & 14% p-wave (dotted) versus scattering angle θ. (b) Velocity distributions for 2 colliding atoms with relative velocity v_r for the differential cross-sections in (a). For the "s + 14% p" (dotted) curve, the scattering is constructive in the forward direction whereas for "s - 14% p", the scattering is constructive for $\theta = 180°$.

velocity is then $v_r = \Delta T \times g$ where ΔT is the launch delay. Here, $\Delta T = 7$ ms $\rightarrow 20$ ms corresponds to collision energies of 19 to 150 μK. This range of energies is interesting as one expects to see the p-wave quantum scattering threshold – at low energies only s-wave scattering occurs[7] since, for impact parameters that are within the range of the interatomic potential, the velocity is low enough that the angular momentum is less than $\hbar$. As the energy increases, there is eventually enough angular momentum for small impact parameters that the ℓ=1 wave scatters.[8]

We use our double-MOT[7] to juggle the atoms. To be sensitive to the differential cross section, we detect the vertical velocity component of the scattered atoms using a 2-photon Raman transition.[7,9] If we neglect the 3-3.5 μK temperature of each ball of atoms, the vertical velocity distribution of the atoms $n(v_z)$ is proportional to $d\sigma/d\Omega(\theta=\cos^{-1}(v_z/v_r)$ where θ is the center-of-mass scattering angle. Therefore, for s-wave (ℓ=0) scattering, the observed velocity distribution should be a "square-pulse" as a function of v_z as shown in the solid curves of Fig. 5. For pure p-wave scattering (dashed curves), the velocity distribution is proportional to v_z^2.

When there is both s & p-wave scattering, the scattering is more interesting. Just as for a multipole expansion for radio waves, the total cross section (radiated power) is just the sum of the s, p, ... cross-sections (dipole, quadrapole, ... powers) – there is no interference in the total "radiated power." However, in the angular distribution of the "radiated power," the s & p-waves interfere. Because the s & p-waves interfere, the angular distribution of the scattering is sensitive to even a very small fraction of p-wave scattering. The interference term scales as the square root of the p-wave cross section (for small

p-wave scattering) so that a p-wave cross section of 14% of the s-wave grossly distorts the angular distribution of the scattering and the velocity distribution that we detect (Fig. 5.).

In Fig. 6, we show the detected velocity distributions for launch delays from ΔT = 7 to 20 ms corresponding to collision energies from 19 to 150 μK. For this data, the atoms in the first ball are prepared in the $6S_{½}$ $|F=4,m=4\rangle$ state and the second ball is prepared in the $6S_{½}$ $|3, 3\rangle$ state. The state preparation raises the temperature of the atoms to ≈ 3-3.5 μK from a launch temperature of 1.5 μK. The 3-3.5 μK temperature broadens the velocity distributions we detect in Fig. 6 as compared to the velocity distributions for T=0 presented in Fig. 5. It is straightforward to calculate the velocity distributions for non-zero temperature.[7]

The data in Fig. 6. shows a p-wave fraction growing for small collision energies. In Fig. 7., we show the s & p-wave cross-sections as a function of energy. At low energies, the s-wave cross section, which is pure triplet scattering, is proportional to 1/E suggestive of a "zero-energy" triplet potential resonance.[10] We however find that the cross section is significantly below the resonant cross section of λ_{dB}^2/π. Since the s-wave cross-section is given by $\sigma = \lambda_{dB}^2/\pi \sin^2(\delta_0)$, an alternative explanation is that in the range of 4-20 μK, the s-wave phase shift δ_0 is constant (and less than the resonant value of $\pi/2$). Further, such an observation of a constant phase shift less than $\pi/2$ suggests that the triplet scattering length is negative since the s-wave phase shift goes as $\delta_0 = -2\pi a/\lambda_{dB}$ for low energies. Therefore, since scattering phase shifts must decrease at high energies, there must be a region of constant phase when $a < 0$.[11] The size of the scattering length is important in all experiments sensitive to cold collisions but the sign is especially important for BEC experiments since a BEC with a large number of atoms is unstable when $a < 0$.[12] At higher energies, the s-wave cross section decreases to nearly zero indicating a s-wave Ramsauer-Townsend cross-section minimum[13] near 150 μK.

The p-wave cross section increases as the square of the energy for low energies as expected for a p-wave scattering threshold. At higher energies, it begins to rollover again showing a region of constant phase shift. Since the p-wave channel is an admixture of singlet and triplet interactions, we can get a great deal of detailed information about the Cs-Cs scattering at low energies. The s-wave data determines the triplet potential allowing the p-wave to determine the singlet. This is the first experiment to resolve the quantum scattering for atomic partial waves.

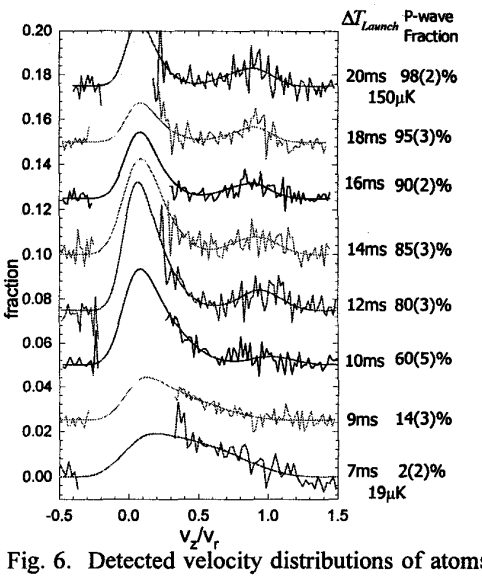

Fig. 6. Detected velocity distributions of atoms in the $|3, 3\rangle$ state colliding with atoms in the $|4, 4\rangle$ state for juggling delays from 7 to 20 ms. The p-wave cross section grows from 2% to 98% of the s-wave.

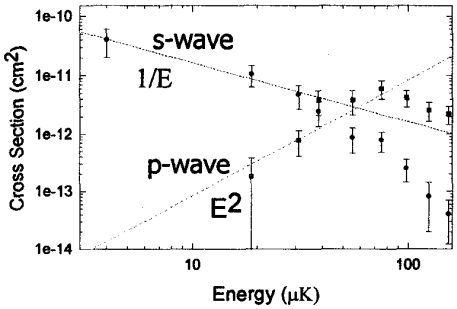

Fig. 7. Energy dependence for s & p-waves for the data in Fig. 6. For reference, we show lines corresponding to 1/E and E^2 corresponding to an s-wave "resonance" and the p-wave quantum scattering threshold. At higher energies, the s-wave cross section goes to zero indicating a Ramsauer-Townsend s-wave minimum near 150 μK.

Conclusion

We have demonstrated a prototype of an ^{87}Rb fountain clock. We have varied the density and

seen a small shift in the clock frequency indicating that the collision shift for ^{87}Rb is at least a factor of 10 smaller than the shift in a laser-cooled Cs clock.

We have demonstrated a juggling Cs atomic fountain where we observed the energy dependence for triplet s-wave scattering and have observed the p-wave quantum scattering threshold and the interference between atomic s & p-wave scattering for the first time. A clock based on a juggling fountain can achieve much higher short-term stability and reduce the requirements of the local oscillator. In a juggling fountain clock, the triplet s-wave cross section that we measure is relevant for collisions between the "opposite" parts of each pair of colliding atoms – i.e. collisions between the $|3,0\rangle$ and $|4,0\rangle$ states are pure triplet interactions. The collision terms between the $|4,0\rangle$ and $|4,0\rangle$ states and the $|3,0\rangle$ and $|3,0\rangle$ states have an admixture of singlet and triplet interactions. The more important collisional process in a juggling fountain clock is the frequency shift cross section. One expects to see similar structures as those presented here. For example, the Ramsauer-Townsend s-wave minimum near 150 μK suggests that it may be optimal to juggle at 50 s^{-1} (or even the next R-T minimum) so that the collisional effects are minimized. With the precise theoretical understanding we are achieving with this data, it should be possible to optimize the design of future juggling fountain clocks.

Acknowledgements

We acknowledge many discussions with Servaas Kokkelmans and Boudewijn Verhaar and financial support from a NSF NYI award, a NIST Precision Measurement Grant, and from NASA.

References

1. E. Tiesinga, B. J. Verhaar, H. T. C. Stoof, and D. van Bragt, Phys. Rev. A **45**, 2671 (1992).
2. K. Gibble and S. Chu, Phys. Rev. Lett. **70**, 1771 (1993).
3. K.Gibble and B. J. Verhaar, Phys. Rev. A **52**, 3370 (1995).
4. S. J. J. M. F. Kokkelmans, B. J. Verhaar, K. Gibble, and D. J. Heinzen, Phys. Rev. A. **56**, 4387 (1997).
5. K. E. Gibble, S. Kasapi, and S. Chu, Opt. Lett. **17**, 526 (1992).
6. E. Simon, G. Santarelli, Ph. Laurent, S. Ghezali, P. Lemonde, and A. Clairon, preceding paper in these proceedings.
7. K. Gibble, S. Chang, and R. Legere, Phys. Rev. Lett **75**, 2666 (1995).
8. See P. S. Julienne and F. H. Mies, J. Opt. Soc. Am. B **6**, 2257 (1989).
9. M. Kasevich, D. S. Weiss, E. Riis, K. Moler, S. Kasapi, and S. Chu, Phys. Rev. Lett. **66**, 2297 (1991).
10. M. Arndt, M. Ben Dahan, D. Guéry-Odelin, M. W. Reynolds, and J. Dalibard, Phys. Rev. Lett **79**, 625 (1997).
11. Servaas Kokkelmans has performed detailed calculations describing this behavior, private communication, 1998.
12. See C. C. Bradley, C. A. Sackett, and R. G Hulet, Phys. Rev. Lett. **78**, 985 (1997); C. C. Bradley, C. A. Sackett, J. J. Tollett, and R. G Hulet, Phys. Rev. Lett. **75**, 1687 (1995).
13. Ramsauer, Ann. der Physik **72**, 345 (1923); Townsend and Bailey, Phil. Mag. **43**, 593 (1922).